NUMERICAL MODELLING AND SIMULATION OF HYDROGEN AND AIR MIXING TO PREVENT IGNITION DELAY AND FLASHBACK

by

Marc JAEGER*, Matjaž HRIBERSEK, Filip KOKALJ, Matej ZADRAVEC, and Niko SAMEC

Faculty of Mechanical Engineering, University of Maribor, Maribor, Slovenia

Original scientific paper
https://doi.org/10.2298/TSCI230529250J

Practically all residential and commercial gas appliances installed within the EU today were designed for operation with natural gas. A clean and efficient solution for heating and hot water generation is the combustion of hydrogen in case of a gas condensing boiler. Safe and stable combustion of hydrogen is a complex issue, and several influence parameters must be understood for the safe design of hydrogen capable gas condensing boilers. In premixed hydrogen-air combustion, there are two physical problems that should be avoided at all costs: flashback through the burner to the premixing duct and ignition delay in the combustion chamber. Well mixing of reactants is therefore, very important to achieve stable and efficient hydrogen combustion. To evaluate the influence of commercialized mixing stages (fan-venturi combination), the impact of the rotational velocity on the degree of mixing in case of a venturi-fan combination used in domestic gas condensing boilers is presented in this paper. Transient, 3-D simulations with different turbulence modelling approaches were performed to assess the degree of mixing upstream the hydrogen capable multi-hole burner. It is shown that the lower angular velocities produce better mixing. It can also be assumed that a local variation of up to 17% in the adiabatic flame speed can be expected due to the mixing processes as the consequence of the local air-fuel equivalence ratio variation.

Key words: *CFD, hydrogen combustion, mixing, flashback, gas condensing boiler*

Introduction

In Europe, natural gas is the second most important primary energy source (after oil) today [1]. Hydrogen is expected to play an important role in future energy supply, *e.g.*, as an admixture gas in natural gas grids or in pure condition [2]. Since gases are usually distributed in larger grids and are not limited to certain applications, the supply of hydrogen blends as well as pure hydrogen always concerns a variety of applications: *e.g.*, gas stoves, gas turbines, industrial burners, gas condensing boilers, and many more. As a rule, the gases are burned to produce heat or generate other forms of energy from them. An advantage of *e.g.*, pure hydrogen in burning situations is that there are no emissions of CO_2, which is identified as one of the major GHG. Practically all residential and commercial gas appliances installed within the EU today were designed for operation with natural gas [2]. Hydrogen combustion in case of a gas condensing boiler can be a clean and efficient solution for heating and hot water generation.

* Corresponding author, e-mail: marc.jaeger@student.um.si

Domestic gas boilers are usually designed as fully premixing systems. The major drawback of lean premixed hydrogen-air combustion is that flammable gas mixtures prevail in regions upstream of the combustion chamber, respectively, the perforated burner. This leads to the risk of flame propagation of flame flashback into the premixing section of the device. As the premixing section is not designed for high temperatures and pressure peaks, flame flashback can cause critical damage to the heating device. There are five different types of flashback [3]: turbulent flame propagation in the core flow, boundary-layer flashback, combustion induced vortex breakdown – occurs only in swirl stabilized burners, flashback due to combustion instabilities, and flashback due to auto ignition.

First theoretical achievements regarding flame stability of premixed flames were done by Lewis and von Elbe [4] and later by von Elbe and Menster [5] for premixed methane and hydrogen-air flames, respectively. They developed the so-called theory of 'critical velocity gradient' which is very well known in literature with respect to boundary-layer flashback. The investigation of flame stability is still an important field of research today. Baumgartner *et al.* [6] experimentally studied the flashback behavior in unconfined premixed flames supplied by a channel flow. It was demonstrated that the current critical gradient model does not accurately consider the shape and position of the stable, unconfined flow. The tendency for flashback is primarily determined by the flame speed and the heat transfer between the flame base and burner rim. Vance *et al.* [7] conducted detailed numerical investigations into flashback phenomena of hydrogen-air premixed flames stabilized on multi-slit burners by varying excess air and geometrical parameters of the burner configuration. With the help of the gained results, they extended the flashback correlation of Lewis and Elbe for Lewis-numbers less than one to consider preferential diffusion the flame front. Miguel-Brebion *et al.* [8] studied the effect of flame holder temperature on flame-stability of a laminar premixed flame on cylinder. They concluded that the conjugated heat transfer between flow and solid has a major effect on the flame topology. In their study on a full-scale model of an industrialized gas condensing boiler, Henrichs *et al.* [9] found a significant variation in burner outflow velocities, which resulted in varying flame lengths and inhomogeneous burner temperatures. The modulation range is restricted due to its influence on flame stability.

Normally, when *e.g.*, methane is freely diffused in the air, it takes a long time to mix evenly. Therefore, the gas and air need a sufficiently long mixing distance in the state of absolute flow. But the long mixing distance cannot exist in residential heating device in [11].

Hydrogen gas is compared to methane or natural gas highly diffusive and highly buoyant; it rapidly mixes with the ambient air upon release. Hence, a currently unquantifiable improvement of the mixing quality is to be expected. The propagation of a chemical reaction can only take place under limited mixing ratios of air and hydrogen and depends also on the velocity field as well as on the mixing procedure of fuel and oxidizer [10]. Hydrogen-air mixtures have high flame speeds compared to many other fuels – factor eight under stochiometric conditions compared to methane-air combustion. Thereby, the laminar burning velocity is defined as the velocity at which unburned gas of a given composition, pressure, and temperature flows into a flame in direction normal to the flame surface. The normal direction is specified to make the velocity independent of its shape [11]. Hermanns published a collection of experimental determined burning velocity hydrogen-air flames at ambient conditions known in the literature, see fig. 1.

The flame stability of premixed hydrogen combustion is influenced by several factors, and the mixing quality of hydrogen and air is a crucial aspect. The mixing quality refers to how well hydrogen and air are blended before combustion. In the following, there are additional key

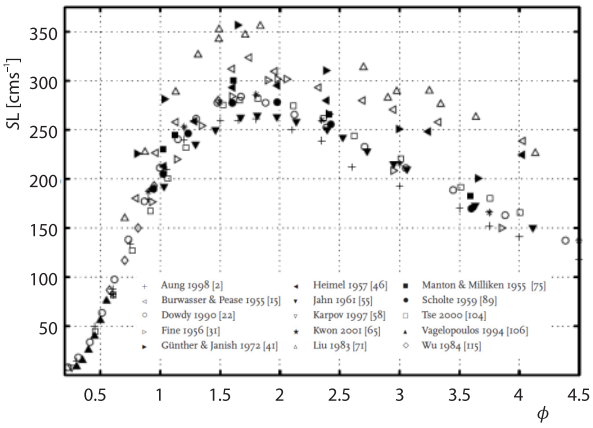

Figure 1. Collection of different experimental results from the Hermanns [12] Ph. D. thesis of the adiabatic burning velocity of hydrogen-air flames at ambient conditions

considerations except the flame speed, which should be considered in case of mixing quality estimation, important for achieving the stable premixed hydrogen combustion:

– Hydrogen has a wide range of flammability, *i.e.*, it can burn over a wide range of concentrations in air. The quality of the mixture should ensure that the mixture falls within these limits for stable combustion.
– Proper mixing is essential for uniform distribution of hydrogen within the air mixture. Inhomogeneous mixing can result in areas of higher or lower concentration, affecting ignition. Conversely, poor mixing can also lead to quenching, where the mixture falls below the lower flammability limit and combustion cannot be sustained.
– The quenching distance is the distance over which a flame can propagate before being extinguished. Proper mixing can affect this distance, with better mixing reducing the risk of quenching.

However, the quality of mixing between hydrogen and air is critical for flame stability in premixed hydrogen combustion. It influences factors such as flammability limits, ignition, quenching, flame speed, turbulence, quenching distance, and the risk of lean or rich flashbacks. Optimizing mixing conditions is essential for achieving stable and efficient hydrogen combustion.

Zhang *et al*. [13] and Liu *et al*. [14] deal with the optimisation of mixture quality using the example of real systems. Both studies attribute a corresponding relevance to the mixing quality regarding emissions from premix burners. However, they deal with so-called nozzle mixing systems in which the fuel is only fed after the blower with oxidiser.

The main objective of this study is to evaluate the degree of mixing, which is crucial for stable and safe combustion in future hydrogen capable gas condensing boilers. Most previous presented studies have assumed a completely premixed mixture in their investigations, which is why a corresponding contribution is to be made here. The study, based on the example of an industrialized gas condensing boiler, used a mixing stage – presented in the next chapter – which is available on the market and widely used in these appliances. In fact, it is difficult to assess the mixture quality at the outlet of the blower studied due to its compact design. Therefore, a numerical approach is used in this study.

The key novelty of this study can be summarized as:

– A comprehensive numerical model is applied, incorporating all significant effects, including the rotation of the impeller mesh, thermal mixing modelling, advanced turbulence models and a genuine series blower, which is utilized in commercially available gas condensing boilers.

– A grid independence study has been carried out and validated with measured values from experiments.
– Angular velocities and turbulence models are varied at a defined excess air value to investigate and evaluate the degree of mixing of the fan and to draw conclusions about the influence on flame stability.

Methods

The CFD simulation

Due to the compact design of gas boilers, especially of the assembled components, it is very difficult to measure local flow variables as well as substance concentrations. In particular, invasive measurement methods could have a considerable influence on the flow behaviour, whereas optical measurement methods would be conceivable, but were out of the question due to the technical measurement effort involved. To evaluate the influence of the degree of mixing on flame stability of a hydrogen capable gas condensing boiler compared to common methane combustion, numerical simulations were performed. The mixing stage consists of three components, namely a radial fan with an integrated venturi and a gas valve regulating the burnable gas volume flow, see fig. 2.

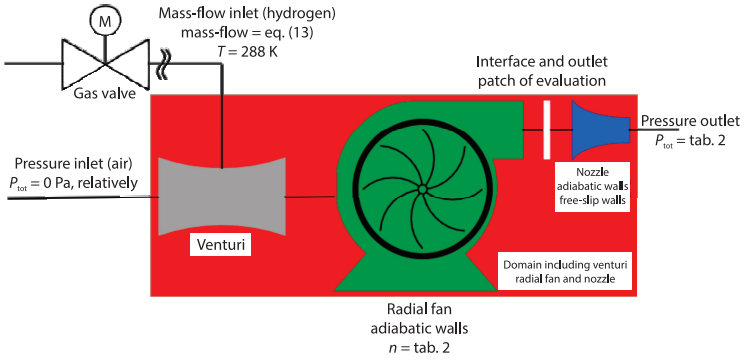

Figure 2. Overview of different cell zones and boundary conditions of the mixing stage

The investigated assembly is an industrialized product, which cannot be geometrically simplified. Hence, it must be treated generically as a 3-D simulation be able to calculate the degree of mixing as realistically as possible. The investigated problem is a three-component mixture, namely nitrogen, oxygen, and hydrogen. Furthermore, the burnable gas is supplied with a temperature of 288 K where the combustion air is supplied with a temperature of 323 K. Thus, there is a volumetric heat exchange between the components. This was treated by solving the energy equation. Modelling of mixing and transport of chemical species by conservation equation can be done with ANSYS FLUENT describing convection, diffusion, and reaction sources for each component species. For non-reacting system with multi-components the balance equations for the mass conservation, the momentum, and the energy as well as the mass of each species is to be solved.

Simulation domain and grid

The fan is designed for a 32 kW gas condensing boiler and is applied in a 15 kW device. The nominal rotational speed of the radial impeller is 14000 rpm, however in the 15 kW application the nominal flow for 14 kW heat input is reached at 9500 rpm – for G20, pure meth-

ane according to EN 437 [15], and 5% excess air. Another important property is the amount of main and splitter blades for the definition of the transient time step: the impeller is characterized by 11 main and 11 splitter blades – hence, 22 blades in sum.

As depicted in fig. 3 the numerical outlet face is shown in red and the small blue circular area is the gas-inlet as well as the big blue circular area is the air inlet. Additionally, the grey surface represents a non-slip wall, excepted the surface of the nozzle, which is added downstream the fans volute.

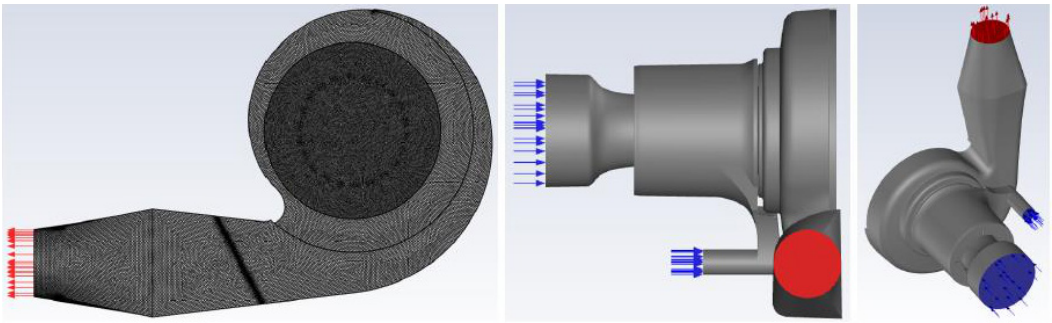

Figure 3. Illustration of the simulated and simplified model

The nozzle is needed to stabilize the simulation. Pre-calculations showed that there is a very non-homogenous and transient velocity distribution at the outlet of the volute. There were a lot of re-circulation areas in the vicinity of the fans outlet, which results in a numerical instability. To reach a lower level of residuals it was necessary to accelerate the flow without significantly influencing the total pressure.

At this point it is important to note that all shown results in this paper are results in from the real outlet of the fan. In other words, the aforementioned nozzle is only needed for numerical purposes. Figure 2 shows an abstract version of the simulated domain. The white illustrated interface corresponds to the real outlet of the fan.

The domain dimensions are 193 mm in x-direction, 129 mm in y-direction, and 124 mm in z-direction, respectively. The mesh was generated by using the ANSYS FLUENT Mesher, while the volume mesh corresponds a polyhedral mesh. Since this is a complex 3-D geometry close to series production, it turned out during the mesh generation process that the polyhedral mesh achieves the highest mesh quality. The corresponding geometry can be seen in fig. 3. The mesh complies with the quality requirements of the ANSYS FLUENT user guide [16]. A maximum volumetric cell length of 1.5 mm was used for the coarsest grid. In addition the volumetric cell length, the face cells for the finer resolutions were also reduced by grid refinement factors of approximately 1.3 using the grid convergence (GCI) method.

Modelling close to the wall has a significant impact on the accuracy of the numerical solutions, as the walls are the main source of mean vorticity and turbulence. To ensure that the boundary-layer is solved with the highest accuracy, a fixed first cell height of 0.01 mm was defined for all three meshes in the grid independence study. This ensured that y^+ was always less than one. Since all three different turbulence models used in this study (statistical RANS model: SST k-ω, statistical URANS model: SST k-ω and hybrid URANS/LES: DDES) are treating the near-wall area with the k-ω model, ANSYS recommends a near-wall treatment of ω-based turbulence models of y^+ less than one. In order to check the accuracy of the turbulence models, among other things, model comparisons were carried out in the further course.

Characteristic properties of the fan

To evaluate the fans performance, it is necessary to introduce two important characteristic properties of the fan.

Total pressure increase

It can be reasonably assumed that the most significant variable is the increase in total pressure in the mixing stage. The mixing stage is provided by the supplier and has been developed for use in gas condensing boilers. The *P*-*V*-characteristic curve was determined experimentally by the supplier. These measurement outcomes were employed to calculate operating points and subsequently to validate the simulation results. In the mentioned experiment, the assembly sucks in the air from the environment. Since there is no change in energy, it can be derived from Bernoulli equation that the total pressure is constant between ambient and venturi inlet ($P_{\text{tot,ambient}} = P_{\text{tot,inlet venturi}}$). Furthermore, the fan flows into a large volume within the experimental framework, where the flow velocity can be assumed to be zero. Hence, according to Bernoulli, the total pressure at the interface between the nozzle and the volute is the same as the total pressure measured in the box. Thus, it results in the correlation:

$$\Delta P_{\text{tot,tot}} = P_{\text{tot,2}} - P_{\text{tot,1}} = P_{\text{tot,interface}} - P_{\text{tot,inlet venturi}} \tag{1}$$

The Z-moment

The total moment vector about a specified center *A* is computed by summing the cross products of the pressure and viscous force vectors for each face with the moment vector $\vec{r}_{AB}$, which is the vector from the specified moment center *A* to the force origin *B* [16].

The terms in this summation represent the pressure and viscous moment vectors:

$$\vec{M}_A = \vec{r}_{AB} \times \vec{F}_P + \vec{r}_{AB} \times \vec{F}_{Visc} \tag{2}$$

Since the pressure forces around the axis of rotation almost neutralize each other in a centrifugal fan – except for the potential interaction of the inhomogeneous pressure distribution of the volute on the impeller – the viscous forces dominate the moment around the axis of rotation at this point. To represent the shear forces, this parameter is selected for the applicated GCI method.

Mixing efficiency in single-phase multicomponent flow

To be able to evaluate the degree of mixing it is from elementary importance to have a variable which represents the mixing efficiency of the mixing stage. Based on the idea of Weltens *et al*. [17] who formulated an index to evaluate the uniformity of flow velocity at the cross-section of a catalytic gas converter and the evaluation of Thienthong *et al*. [18] who have compared five commonly used mixing indices, a uniformity index for the degree of premixing, *UIpre*, adapted to the problem at hand was defined. An area weighted *UIpre* is inserted, normalised from 0 to 1 – where 0 corresponds to completely unmixed and 1 to perfectly premixed. Since a non-uniform mesh is used at the volute's outlet, an area weighted uniformity index is important. Hence, the area averaged mole fraction of hydrogen can be calculated:

$$\overline{y}_{\text{H}_2} = \frac{\sum_{i=1}^{N} y_{\text{H}_2,i} \cdot A_i}{A_{\text{out}}} \tag{3}$$

where $y_{H_2,i}$ is the hydrogen mole fraction in cell i, A_i – the surface area of cell i, and A_{out} – the integral area of the outlet surface. The local non-uniformity index ω_{H_2} is defined:

$$\omega_{H_2,i} = \frac{\sqrt{\left(y_{H_2,i} - \overline{y}_{H_2}\right)^2}}{\overline{y}_{H_2}} \tag{4}$$

and represents the difference between the local mole fraction and the averaged mole fraction referenced by the evaluated area. The non-uniformity index, ω, of the mole fraction passing through a control surface is defined:

$$\overline{\omega} = \frac{\sum_{i=1}^{N}\left(\omega_{H_2,i} \cdot A_i\right)}{A_{out}} \tag{5}$$

Thus, the degree of premixing *UIpre* can be calculated with the equation:

$$UIpre = 1 - \frac{\overline{\omega}}{2} \tag{6}$$

According to the definition, *UIpre* could be as high as 1, when the hydrogen mole fraction in the zone of interest is completely uniform, *i.e.*, $y_{H_2,i} = \overline{y}_{H_2}$ everywhere in the zone. For example, *UIpre* = 0.5 indicates that half of the control surface has a mole fraction of 0, while the remaining half experiences double the average mole fraction.

Integral combustion calculation

The premixing stage is to be used to mix fuel and oxidiser – specifically hydrogen and air. To be able to define the inlet conditions a rough understanding of the combustion calculation is necessary. In general, the global reaction mechanism of hydrogen and air under stoichiometric conditions can be illustrated:

$$H_2 + 0.500O_2 + 1.881N_2 \rightarrow H_2O + 1.881N_2 \tag{7}$$

The reaction does not consider the chemical equilibrium and the formation of pollutants like NO_x. To calculate the conversion of substances as a function of the physical power of the device, the global reaction equation is to be formulated in function of the quantity of substance and the mole fraction, considering the excess air:

$$n_{fuel}H_2 + \lambda\left(n_{O_2}^{min}O_2 + \frac{y_{N_2}}{y_{O_2}}n_{O_2}^{min}N_2\right) \rightarrow 0.5n_{fuel}H_2O + \left(\lambda - 1\right)n_{O_2}^{min}O_2 + \lambda n_{O_2}^{min}N_2 \tag{8}$$

The stoichiometric oxygen requirement can be calculated:

$$n_{O_2}^{min} = \left(C + \frac{H}{4} + S - \frac{O}{2}\right)n_{fuel} \tag{9}$$

where the capital letters are the number of chemical elements in the fuel and nfuel [mol] is the amount of fuel substance. The λ defines the ratio between the actual amount of oxygen to the stoichiometric oxygen requirement. In order to determine the inlet mass-flows for the boundary conditions, the calorific value, H_u , known from the literature is required. The lower heating value, respectively the enthalpy of formation at 15 °C for hydrogen is H_u = 241.719 kJ/mol (according to DIN EN ISO 6976). Assuming an excess air of λ =1.3, the mass-flows result for a physical unit power of 14 kW.

In tab. 1. the inlet conditions for pure hydrogen/air combustion at $\lambda = 1.3$ and 14.0 kW heat input are presented:

Table 1. Inlet conditions for pure hydrogen/air combustion at $\lambda = 1.3$ and 14.0 kW heat input

Substance	Mass-flow [mols^{-1}]	Mole fraction [–]
Hydrogen	0.0578943	0.2442
Stoichiometric oxygen requirement	0.0289471	–
Actual amount of oxygen	0.0376313	0.1587
Actual amount of nitrogen	0.1415653	0.5971

Boundary conditions

Since concrete measurement data regarding a hydrogen-capable burner were not known at the beginning of this study, it was assumed that the methane burner used so far is suitable for the combustion of hydrogen. Thus, it was possible to determine a real operating point via the similarity laws of turbomachinery. The *p-V* diagram is available for pure aur with a density of $\rho_1 = 1.2$ kg/m³. If the density of the medium changes to ρ_2, the characteristic curve values change as follows.

For constant angular velocity, the supplied volume flow is constant – assuming that there are no unsteady flows or detachment phenomena in the fan:

$$\dot{V}_{H_2+air} = \dot{V}_{air} \tag{10}$$

The total pressure increase can be calculated:

$$\Delta P_{tot,H_2+air} = \Delta P_{tot,air} \frac{\rho_{H_2+air}}{\rho_{air}} \tag{11}$$

If $\lambda = 1.3$ is constant, the specific gas constant ($R_j = 372.87$ J/kgK) can be calculated from the mass fractions ($w_{H_2} = 2.21\%$ and $w_{air} = 97.79\%$) and the density of the hydrogen-air mixture $\rho = 0.854$ kg/m³ can be determined with the help of the general gas equation. For the calculation, a *Weishaupt* calculation tool was used to determine the mole fraction of reactants as well as the reactants mass-flows. From the similarity laws, the total pressure increases can then be determined for the different rotational velocities. The results can be seen in tab. 2.

Table 2. Total pressure increases for three angular velocities

Angular velocity [rpm]	$\dot{m}_{air+H_2}$ [mols^{-1}]	$\Delta P_{tot,tot}$ [Pa]
9500	4.8074	703
8000	4.0483	499
5000	2.5302	194

In addition, the assumption can be made that a total pressure of 0 Pa prevails at the venturi inlet – this can be derived via the Bernoulli equation. The gas inlet condition can be derived:

$$\dot{m}_{H_2} = \frac{M_{H_2}}{M_{air}} \dot{m}_{air} c_{O_2} \frac{2}{\lambda} \tag{12}$$

Supplemented with the values:

$$\dot{m}_{H_2}^{n+1} = \frac{2.016 \text{ kg/kmol}}{28.966 \text{ kg/kmol}} \dot{m}_{air}^{n} 0.21 \frac{2}{1.3} \tag{13}$$

where $\dot{m}$ is the inlet condition at the subsequent time step in form of the hydrogen mass-flow. This value is based on the solution of the air inlet mass-flow of the previous time step. This was implemented to ensure that the system operates at a constant λ.

Tables 2 and 3 together represent the boundary conditions of the simulations. Table 2 shows the studied operating points whereas the latter table shows the generally valid boundary conditions. The air inlet, in other words the entrance of the venturi, is assumed for the initialisation be a total pressure of 0 Pa. This corresponds the ambient conditions of the fan. Furthermore, the fan is basically mounted inside a gas tide housing, in the in the immediate vicinity of a hot boiler. This results into a preheating of the supplied air. Hence, it is to be assumed that the ambient air is preheated with 323 K. As already mentioned, the gas inlet is defined as a mass-flow inlet, which is updated every calculated time steps by applying the eq. (13) – it follows a constant amount of excess air with respect to the combustion process.

Table 3. Summary of boundary conditions

Boundary/cell zone	Condition	
Inlet air	Pressure inlet	$P_{tot,ini}$ = 0 Pa, T = 323 K
Inlet hydrogen	Mass-flow inlet	T = 288 K, eq. (13)
Outlet	Pressure outlet	$P = cf$ [Pa], tab. 2
Counter rotating wall	Rotational wall	$n = -cf$ [rpm], tab. 2
Nozzle wall	Slip	
Impeller	Rotational domain	$n = cf$ [rpm], tab. 2

The outlet pressure (outlet nozzle) is defined as total pressure according calculated estimated values illustrated in tab. 2. Normally, there is no nozzle applied downstream the origin outlet of the fan. Due to the diverging and generic form of the volute, the flow tends to build re-circulation areas in the actual outlet of the fan. In order to stabilise the simulation numerically, an artificial nozzle was therefore, modelled at the outlet. The wall was modelled as a slip wall to prevent a contribution the pressure increase of the system. As this did not result in a change in the total pressure, the same total pressure can be used at the outlet of the nozzle as is normally used at the actual outlet of the fan. This measure ensured numerical stability and allowed the solver to converge at each time step. Finally, the angular velocity of the impeller's domain was defined according to the values listed in tab. 2.

Governing equations are solved using the commercial code ANSYS FLUENT [19] using a steady and coupled solver for the RANS simulation and an implicit transient and coupled solver applying a fixed time step for the URANS and hybrid RANS/LES simulations. The fixed times step was calculated with 40 time-steps per period, whereas one period corresponds the time of the elapsed time passes until the next main blade is in the same position – in our case this corresponds to an angle of 32.72° and exemplary for 9500 rpm a time difference of $5.7 \cdot 10^{-4}$ seconds. Pressure equation, advection scheme and the equations of the species are solved in second order discretization – the time discretization scheme for the transient simulations was also solved in second order. Gravitational, and viscous work effects are not modelled as they were found not to play the major role.

Model validation

In this section the results of the grid convergence study, including the application of the GCI method [20] to evaluate the numerical error, is presented. First characteristic value of interest is the total pressure increase of the fan with a defined mass-flow rate. Due to the slightly fluctuating values, the calculated values were averaged over 1000 time-steps to represent the values as accurately as possible - this is true for all three represented values. In tab. 4 the results of the total pressure increase as well as the calculated numerical error in relation the extrapolated value $e_{\text{ext}}^{\text{num}}$ as a function of the amount of mesh cells are depicted.

Table 4. Results of RANS simulations with frozen rotor approach - total pressure increase

Designation	6.0 mio. cells	13.5 mio. cells	31.5 mio. cells
$\Delta P_{\text{tot,tot}}$	904.87 Pa	912.01 Pa	913.38 Pa
$e_{\text{ext}}^{\text{num}}$	0.97%	0.17%	0.03%

Besides the total pressure increase, the moment around z-axis was monitored and evaluated. The results are depicted in tab. 5. As with the calculation results for the total pressure increase, there is almost no difference in the results for the calculated moment.

Table 5. Results of RANS simulations with frozen rotor approach – torque *Z*-axis

Designation	6.0 mio. cells	13.5 mio. cells	31.5 mio. cells
Torque Z-axis	–0.010440 Nm	–0.010443 Nm	–0.010455 Nm
$e_{\text{ext}}^{\text{num}}$	0.07%	0.04%	0.03%

Compared to the potential effects, the difference in numerical error is even smaller for the shear stress dominant torque. This can be attributed to the fact that a $y^+ < 1$ was forced in all simulations – this was implemented by a fixed defined absolute first layer thickness in the boundary-layer. This first layer thickness was left the same for all meshes.

Figure 4 shows the distribution of velocity vectors over the outlet of the volute. The maximum velocity was used as an indication of a local flow variable.

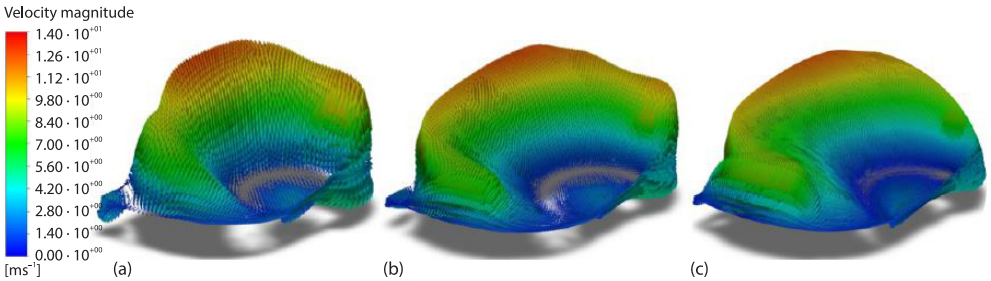

Figure 4. Maximum velocity at the volutes outlet – grid convergence study; (a) 6 mio cells, (b) 13.5 mio cells, and (c) 31.5 mio cells

Compared with the before mentioned parameters, the numerical error is lower than 1%, see tab. 6. for all mesh sizes. However, it can also be determined that the fine mesh resolutions depict the characteristics of the small velocity vectors more accurately.

It can be summarised that all three meshes represent the selected flow variables very well regarding the numerical error. As the mixing simulations are computationally intensive

because of moving mesh approach, hybrid RANS/LES turbulence model and non-reacting single phase multi-component simulation, the mesh with 13.5 mio. cells were used for further simulations. As already mentioned, the numerical error is very low for all three simulated mesh sizes for the application of the GCI method – adequate numerical results were achieved: total pressure increase -integral value-, maximum velocity -scalar-, moment around *z*-axis -shear dominated force-).

Table 6. Results of RANS simulations with frozen rotor approach – maximum velocity outlet of the volute

Designation	6.0 mio. cells	13.5 mio. cells	31.5 mio. cells
abs($v_{max,out}$)	12.46 m/s	12.40 m/s	12.38 m/s
e_{ext}^{num}	0.97%	0.17%	0.03%

To evaluate the accuracy of different turbulence models, four different approaches were investigated. Table 7 shows the results of the following simulations: steady-state regime with and without interface, transient regime with statistical turbulence model and hybrid model as well as the measurement results from the test.

Firstly, when comparing the total pressure increase, the difference between connected and non-connected mesh is < 0.2%. If one compares the simulation results of steady-state and transient, a considerable difference is noticeable.

Table 7. Total pressure increase – comparison of the turbulence models and the measured data

Cases	RANS connected mesh	RANS	URANS	Hybrid RANS/LES	Experiment
$\Delta P_{tot,tot}$ [Pa]	912.09	913.81	954.19	952.78	939.42

There are a few limitations of the frozen rotor model that could lead to the large deviation. The frozen rotor model ignores the relative motion of the fluid zone with respect to each other, and thus do not account for fluid dynamic interaction between the components. It means, that the results may be depended on the frozen position of the component. Nevertheless, the transient approach gives a very good result. The relative difference between the measured date (according to the supplier: measurement error 1%) is approximately 1.5%. It can therefore, be summarised that the transient models with this mesh size represent experiment very well.

Figure 5 shows the comparison of the velocity magnitude in the cross-section of the volute. In the area of the impeller and the interface, there is nearly the same magnitude of the velocity. In the area of the pressure recovery, there is a significant difference of the flow behaviour. Whereas the pure statistical turbulence models RANS and even URANS show a smoothed and smeared magnitude velocity, the hybrid RANS/LES approach clearly shows the vortices of the natural flow behaviour.

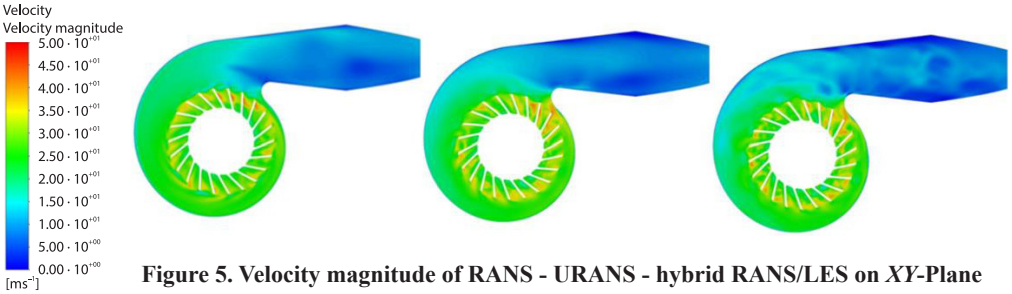

Figure 5. Velocity magnitude of RANS - URANS - hybrid RANS/LES on *XY*-Plane

In summary, it can be said that especially the non-stationary regimes provide very good results – in terms of the selected fan characteristics. Since the next step will be to evaluate the mixing behaviour of the fan, the requirements to the turbulence model probably will change significantly. The anisotropy of the large-structure eddies could play a significant role in the quality of the premixing.

Results and discussion

In this chapter the results of the parameter study are presented. The following parameters were varied to gain an impression of their sensitivity regarding the mixing behavior: Turbulence models (statistical RANS model, statistical RANS model with transient solution approach URANS and hybrid RANS/LES approach DDES) and rotational speed (5000 rpm, 8000 rpm, and 9500 rpm). The different turbulence models also require different approaches to the modelling of the rotating systems. In addition mass transfer (mixing of hydrogen and air), the influence of heat transfer on the mixing behavior was also investigated. For this, different gas temperatures were assumed (T_{gas} = 288 K and T_{air} = 323 K). This also corresponds to real operating points because the supplied gas is usually transported in the ground and comes out of the pipe at approximately 15 °C, while the combustion air is usually transported in the ground. The simulations were carried out under the assumption that the required volume flow does not change when the required medium is changed. From this, it was possible to estimate the required mass-flow and its resulting total pressure increase from the measurement data with pure air via the similarity laws of fans to an air/hydrogen mixture. An important fact is that the similarity laws of fans are only guilty if there are no significant changes in flow conditions *e.g.*, in general no unsteady flow conditions including: eddy separation, flutter, surge, rotating stall, flow separation and transient operation. However, it can be assumed that the flow triangles of the turbomachine will change significantly due to the changing viscosity and density of air of an air/hydrogen mixture with the result of a change in the operational point, respectively the pumped mass-flow. For the simulations with pure air using the GCI method, air was used at a molecular and constant viscosity of $1.837 \cdot 10^{-5}$ kg/ms. Compared to the constant molecular velocity of the hydrogen-air mixture: $1.720 \cdot 10^{-5}$ kg/ms. Furthermore, the density changes from pure air 1.1400 kg/m³ to the mixture's density of 0.8984 mg/m³, where the density pure hydrogen is 0.0819 kg/m³. Therefore, it can be assumed that a change in the operating point is to be expected here.

Integral values

First, characteristic properties of the fan are to be compared. Figure 6(a) shows a comparison of the total pressure increase between venturi inlet and volutes outlet with different angular speeds and using three different turbulence model approaches. The different approaches provide comparable results. There are no significant differences regarding this integral flow property. Once can be seen that the pressure increase slightly arises considering the inherent unsteady flow regime and in the second step again by calculating the large-scale eddies. This picture is independent of the simulated speed. Presumably, the calculation of the transient large-scale vortices plays a role in the pressure recovery of the volute or the entire mixing stage.

The second property of interest is the mixing efficiency of the whole premixing stage. As introduced the mixing efficiency plays a significant role in the operational range of premixed combustion using a perforated multi-hole burner. The illustrated fig. 6(b) represents the uniformity index as an area weighted value. According to eq. (6) the calculated values are all over 99% degree of mixing. It is well known that turbulence, especially the small eddies of the

energy cascade, plays a significant role in mass transfer, respectively diffusion. Looking at the results, one can see that the different turbulence models show roughly a comparable degree of mixing regardless of the simulated speed.

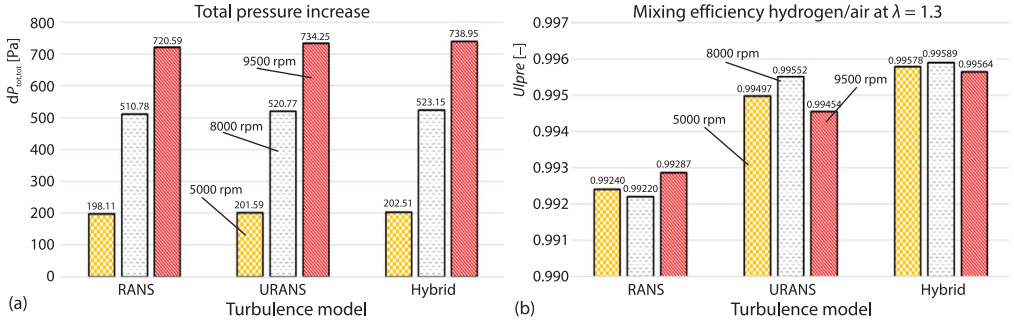

Figure 6. (a) Total pressure increases across the fan as a function of speed and from left to right: RANS, URANS and hybrid RANS/LES (DDES) and (b) *UIpre* according to eq. (6) as a function of speed and from left to right: RANS, URANS, and hybrid RANS/LES (DDES)

It can be said that with the calculation of the inherent unsteady flow behaviour and additionally the large-scale eddies, the area-related degree of mixing increases. In principle, however, the calculated values are very high and are probably not suitable for more detailed analysis.

Local excess air at constant rotational speed

In addition representing the mole fraction of hydrogen for the purpose of evaluating combustion properties, it is more straightforward to convert the property into a local access air quantity λ. This variable can be derived for hydrogen-air combustion $\lambda = \nu_{H_2} y_{O_2}/y_{H_2}$, where ν_{H_2} represents the number of hydrogen elements, respectively the amount of the substance for stoichiometric conditions, y_{O_2} stands for the local oxygen mole fraction and y_{H_2} for the local hydrogen mole fraction, respectively.

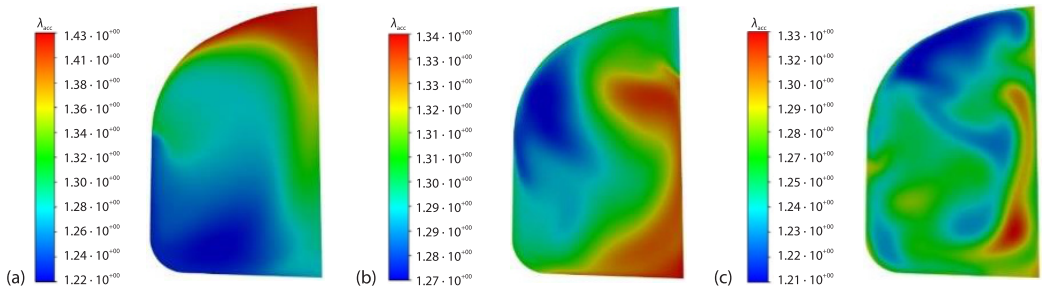

Figure 7. Theoretical local excess air, λ, at 9500 rpm; (a) steady statistical RANS approach, (b) unsteady statistical RANS approach, and (c) hybrid RANS/LES approach

Referenced to the minimum λ value the range of λ is <20 % for all turbulence models and all of them are in the lean range, see fig. 7. (snapshots of local λ distribution at the volute's outlet). With respect to flashback phenomena this is a good property, fig. 1. shows clearly that the adiabatic flame velocity of hydrogen reaches its maximum at equivalence ration $\Phi = 1.7$, which means that the probability of flashback is the higher the closer the operational point to the maximum. Furthermore, there are no under stoichiometric conditions for all mod-

elled approaches which also means that there will be no stoichiometric conditions upstream the surface of evaluation according to the Second law of thermodynamic. Since there is a mole fraction of 0 to 1 in the whole domain, the mixture is well mixed at the outlet – target λ is the λ defined in the boundary conditions equal to 1.3.

This equals well to the calculated uniformity indices *UIpre*. The fact is that the *UIpre* is very high due to the wide range of possible molecular fractions, considering that it lies between 0 and 1. However, the λ range is quite small, assuming that it ranges from 0 to infinity. However, the calculated range of excess air in the outlet area varies more in reality, which is a large deviation in combustion with respect to the change of adiabatic flame velocity. Therefore, it can be concluded at this point that the *UIpre* may have to be adjusted to display the value more sensitively.

Table 8. Range of local excess air as well as corresponding adiabatic laminar flame speed at outlet area at 9500 rpm

Variables	RANS	URANS	Hybrid RANS/LES
λ_{max} [–]	1.43	1.36	1.33
λ_{min} [–]	1.22	1.21	1.21
$S_{L,\lambda_{max}}$ [ms^{-1}]	1.19	1.32	1.37
$S_{L,\lambda_{min}}$ [ms^{-1}]	1.59	1.61	1.61
ΔS_L [ms^{-1}]	0.40	0.29	0.24
$\Delta S_L/S_{L,\lambda_{1,3}}$ [%]	28.0	20.3	16.8

In order to quantify the calculated values of the local excess air more precisely in relation its effect on flame stability, the excess air is converted to its corresponding theoretical adiabatic laminar flame speed, see tab. 8. Note that the adiabatic laminar flame temperature was calculated by help of the published values in the model fuel library published by ANSYS [21]. The relevant data can be found in the chapter hydrogen-based fuels.

Looking at the ratio of the difference between the adiabatic laminar flame speed at minimum local excess air and maximum excess air to the flame speed at nominal excess air depending on the model used, a variation of approximately 28.0%-16.8% can be expected. Under certain circumstances, this calculated range can significantly restrict the modulation range under limit conditions in stationary operation, as a corresponding influence on flame stability is to be expected. Such fluctuations could also conceivably be the cause of the excitation of thermoacoustic phenomena.

Variation of rotational speed using the hybrid RANS/LES approach

In this subchapter, different operational states, respectively angular speeds are compared and analysed. In the following, the focus will be on the variation of λ at the volute's outlet and additional on the temperature distribution of mixture. Furthermore, the hybrid RANS/LES model is to be shown, because big turbulent eddies are calculated and are independent from statistical approaches. As already mentioned, the mixing procedure depends on degree of turbulence, the concentration gradient, and the diffusion coefficient. It therefore, suggests that like the combustion process, the degree of mixing improves with increasing Reynolds number (in combustion, a higher Reynolds number number can increase the surface area of the flame and thus more material can be converted in diffusive combustion). An increasing Reynolds number goes hand in hand with an increasing rotational speed.

Figure 8 shows the speeds of the impeller decreasing from right to left, the color maps are scaled from the local's minimum value up to the maximum. Given that the averaged air-fuel equivalence ratio is defined as λ equal to 1.3, the local minimum and maximum provide insight into the degree of mixing.

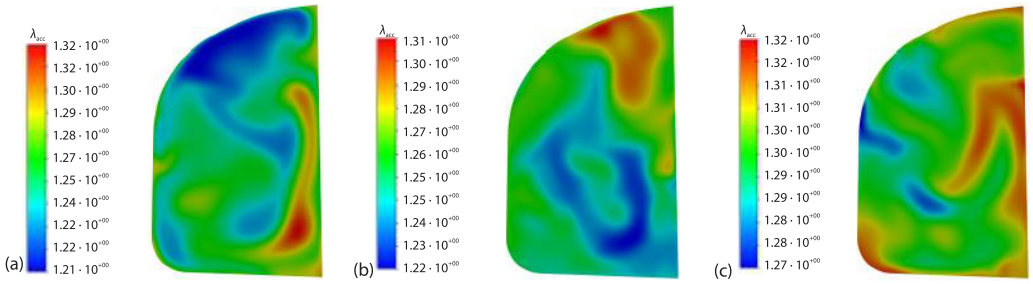

Figure 8. Theoretical local excess air (λ) - hybrid RANS/LES approach

If the instantaneous recordings do not vary significantly in the range of fluctuation over time, it can be said that as the speed or turbulence level increases, mixing becomes less good because the range of fluctuation increases from minimum to maximum. One reason for this could of course be the absence of time for proper mixing or the absence of a mixing path. Looking at fig. 6, it can be said that the mixing quality tends to be better at low speeds and lower turbulence levels than it is at higher speeds and higher turbulence levels. For this reason, the previous chapter focussed on the maximum fan speed, because this operational point represents indeed the worst case.

Ultimately, an examination of the temperature distribution at the outlet as a function of fan speed reveals, as was observed in the preceding chapter, that the mixture is nearly fully mixed with regard to heat transfer. The mixing temperature lies in a range of less than 1 K for all operating points, see fig. 9. If the influence of the thermal mixing due to the temperature gradients in the disturbance on the total mixing degree is small, it may be possible to dispense with solving the energy equation reduce the calculation time.

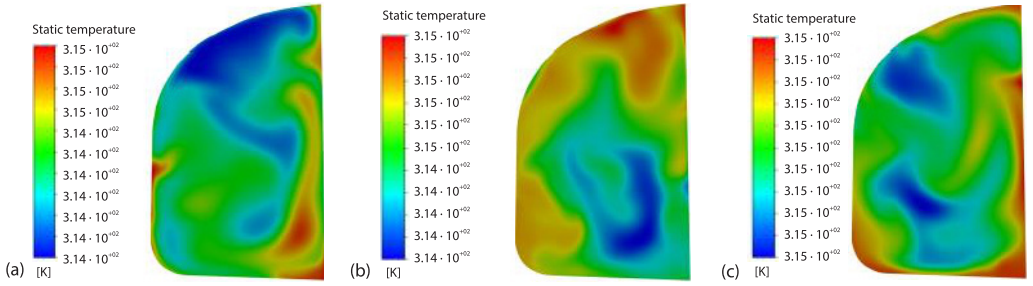

Figure 9. Static temperature at volutes outlet - hybrid RANS/LES approach

In the following, the temporal variation of the local excess air will be discussed. The speed of 9500 rpm with sliding mesh model and hybrid RANS/LES approach is analysed in the following. Two complete rotor revolutions were calculated, and the values were averaged over one complete revolution. The distribution of the λ is represented as an average over time and area in the form of the Gaussian normal distribution at – see fig. 10. The ideal homogeneous mixture is represented by the red vertical line. Green is the time-averaged area minimum of λ as well as yellow is the time-averaged area maximum of λ over a whole simulated revolution.

Additionally, the fluctuation range over time of the averaged, the minimum and maximum λ is shown grey shaded. It can be clearly seen from this illustration that there is a clear variation in the local mixing ratios over time. The exact calculated values of local λ at the left and right limits can be seen in the tab. 8.

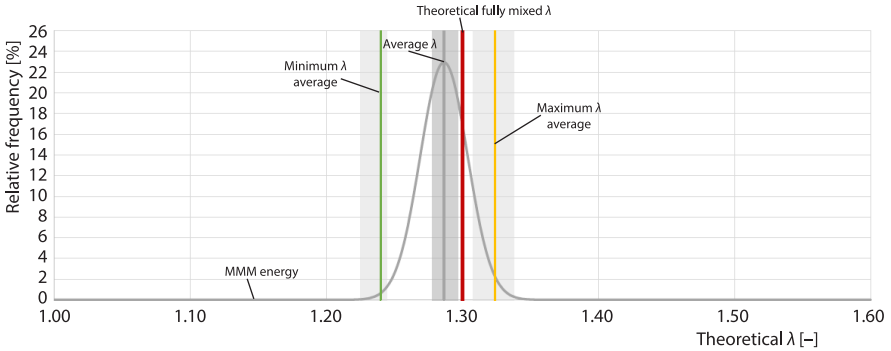

Figure 10. Time-averaged Gaussian probability distribution of the variation of the theoretical λ at the volute's outlet and a rotational speed of 9500 rpm by using the hybrid RANS/LES approach; the fluctuation range of the minimum, maximum and averaged λ over a complete rotor revolution is shown in grey

In addition the minor influences of the temperature differences between the supplied hydrogen and the intake air, the degree of turbulence and the engine speed in particular have a significant influence on the mixture quality and thus also on the theoretical local flame speed. What was not taken into account in this study was the change in the operating point when using a real hydrogen burner. As things stand today, it is assumed that hydrogen burners will have a considerably higher pressure loss compared to the methane burners used to date. The reason for this is the significantly higher adiabatic flame speed, which requires a reduction in the hole diameter, resulting in a higher pressure loss. Due to the lower volume flow, the Reynolds-number and thus the turbulence intensity drops, which may have a negative effect on the mixing quality.

Furthermore, it is important to note, that boundary-layer flash back phenomena are more present at small heat loads. In this study, the focus was primarily on the worst-case scenario. However, future investigations should focus more on the low speed range.

Another point is the estimation of the turbulence intensity at the venturi inlet. It was made on the basis of a fully developed pipe flow, which can certainly have an influence on the calculation result. A turbulence distribution using the example of a real device was not available. However, as turbulence has an influence on the mixing quality, further study work may be necessary here.

Due to the missing manifold, the component between the fan outlet and burner inlet, no final estimate can be made of the influence on combustion. In this area, there may either be further mixing of the gases or segregation due to the large differences in density. An extension of the simulation model with manifold and real hydrogen burner is therefore, part of the future research work.

Conclusions

Well mixed hydrogen and air is of crucial importance for stabile premixed hydrogen combustion. Small ranges of λ deviation may has strong impact on flame stability. This can, of course, have a considerable influence on the operating behaviour of the entire system.

Lower impeller velocities produce a better mixing. Hence, the degree of mixing is dominated by mass diffusion of hydrogen into air and vice versa in comparison turbulent mixing. Comparing the different numerical models, it is concluded that due to the uncertainty regarding the solution dependence on the blade position and the strong sensitivity of the mixture quality and flame speed, the moving mesh model should rather be used in combination with the hybrid RANS/LES turbulence model, as this effect does not occur here.

Furthermore, it can be said that thermal mixing is finished at the end of the mixing stage from a practical point of view. The parameter *degree of mixin*g designed for this study is less useful for further investigations. The remarkably high values do not represent the wider range of locally varying concentrations of hydrogen. Only by looking at the time variation of the local lambda values using the Gaussian normal distribution, the influence of the mixing stage on the degree of mixing was understood more clearly. The most important finding in this context, however, is that the assumption of complete mixing at the burner inlet does not correspond to reality. For future numerical studies investigating flame stability in the context of hydrogen-air combustion using premixing fans, a variation of almost 17% in the adiabatic flame speed or a variation of approximately 0.12 in λ must be taken into account in case of inlet conditions definition.

Finally, it can be summarized that CFD simulations can be very useful in analyzing and optimizing the mixing process of hydrogen and air, which is of crucial importance at the assuring the stable premixed hydrogen combustion conditions.

Nomenclature

A – area, [m^2]
e – error, [–]
$\vec{F}$ – force vector, [N]
H_u – lower heating value, [kWhm^{-3}]
M – moment, [Nm]
$\dot{m}$ – mass-flow, [kgs^{-1}]
n – amount of substance, [molmol$^{-1}_{\text{fuel}}$]
P – pressure, [Pa]
R_j – specific gas constant, [Jkg^{-1}K^{-1}]
$\vec{r}$ – moment vector, [m]
S_L – adiabatic flame speed, [ms^{-1}]
T – absolute static temperature, [K]
Uipre – uniformity index – degree of mixing, [–]
w – mass fraction, [–]
y – mole fraction, [–]

Greek letters

λ – air-fuel equivalence ratio, [–]
ρ – density, [kgm^{-3}]
Φ – fuel-air equivalence ratio, [–]
ω – non-uniformity index, [–]

Subscripts and superscripts

air – air
ext – extrapolated
fuel – fuel
min – minimal
num – numerical
out – outlet
tot – total

References

[1] ***, BP, Statistical Review of World Energy, 2022, 71
[2] Leicher, J., *et al*., Impact of Hydrogen Admixture on Combustion Processes – Part I: Theory, THyGA, Saint-Denis, La Plaine, France 24, 2021
[3] Endres, A.O., Numerical Modelling of Boundary-Layer Flashback in Premixed Hydrogen-Air Combustion Systems, Ph. D. thesis, Technische Universitat, Munchen, Germany, 2020
[4] Lewis, B., Von Elbe, G., Stability and Structure of Burner Flames, *J. Chem. Phys*., 11 (1943), 2, pp. 75-97
[5] Von Elbe, G., Mentser, M., Further Studies of the Structure and Stability of Burner Flames, *J. Chem. Phys*., *13* (1945), 2, pp. 89-100
[6] Baumgartner, G., *et al.*, Experimental Investigation of the Transition Mechanism from Stable Flame to Flashback in a Generic Premixed Combustion System with High-Speed Micro-Particle Image Velocimetry and Micro-PLIF Combined with Chemiluminescence Imaging, *J. Eng. Gas Turbine Power*, *138* (2016), 2

[7] Vance, F. H., *et al*., Development of a Flashback Correlation for Burner-Stabilized Hydrogen-Air Premixed Flames, *Combust Flame*, *243* (2022), 112045
[8] Miguel-Brebion, M., *et al*., Joint Experimental and Numerical Study of the Influence of Flame Holder Temperature on the Stabilization of a Laminar Methane Flame on a Cylinder, *Combust Flame*, *172* (2016), Oct., pp. 153-161
[9] Hinrichs, J., *et al*., The 3-D Modelling Framework and Investigation of Pollutant Formation in a Condensing Gas Boiler, *Fuel*, *300* (2021), 120916
[10] ***, Technische Verbrennung: Verbrennungstechnik, Verbrennungsmodellierung ... - Franz Joos - Google Books (in German), https://books.google.de/books/about/Technische_Verbrennung.html?id=NC4iBAAAQBAJ&redir_esc=y
[11] ***, Survey of Hydrogen Combustion Properties - Isadore L. Drell, Frank E. Belles - Google Books, https://books.google.de/books/about/Survey_of_Hydrogen_Combustion_Properties.html?id=DJ_8GwAACAAJ&redir_esc=y
[12] Hermanns, R., Laminar Burning Velocities of Methane-Hydrogen-Air Mixtures, Ph. D. thesis, Eindhoven Uni. of Tech., Eindhoven, The Netherlands, 2007
[13] Zhang, T. H., *et al*., Optimization of Gas Mixing System of Premixed Burner Based on CFD Analysis, *Energy Convers Manag*, *85* (2014), Sept., pp. 131-139
[14] Liu, F. G., *et al*., On Optimal Design and Experimental Validation of Household Appliance Burner of Low Pollutant Emission, *Energy Convers Manag*, *76* (2013), Dec., pp. 837-845
[15] ***, DIN EN 437 - 2021-07 - Beuth.de, https://www.beuth.de/de/norm/din-en-437/338019127, 2021
[16] ***, Ansys Product Help, https://ansyshelp.ansys.com/account/secured?returnurl =/Views/Secured/prod_page.html?pn=Fluent&prodver=22.1&lang=en
[17] Weltens, H., *et al.*, Optimisation of Catalytic Converter Gas-Flow Distribution By CFD Prediction, SAE Technical Papers, 1993-03-01, 1993
[18] Thienthong, T., *et al*., Mixing-Performance Evaluation of a Multiple Dilution Micro-Fluidic Chip for A Human Serum Dilution Process, *Engineering Journal*, *25* (2021), 9, pp. 67-87
[19] ***, ANSYS Fluent Release 2020R2
[20] ***, Procedure For Estimation and Reporting of Uncertainty Due to Discretization in CFD Applications, *J. Fluids Eng*., *130* (2008), 7, 078001
[21] ***, Ansys Model Fuel Library|Fuel Simulation Models, https://www.ansys.com/products/fluids/ansys-model-fuel-library

Paper submitted: May 29, 2023
Paper revised: September 4, 2024
Paper accepted: October 17, 2024